Radiation Report

INA1H94-SP Single-Event Effects (SEE) Radiation Report

ABSTRACT

Studies were performed to characterize the effects of heavy-ion irradiation on the single-event latch-up (SEL) performance of the INA1H94-SP radiation-hardened, high common-mode voltage difference amplifier. For device qualification, heavy ions with an LET_{EFF} of 75MeV-cm^2 / mg were used to irradiate the devices with a fluence of 1 × 10^7 ions / cm^2. The results demonstrated that the INA1H94-SP is SEL-free up to the specified surface LET_{EFF} = 75MeV-cm^2/ mg at 125°C.

Characterization of single-event transients (SET) and correlation testing of SEL were also performed, up to a surface LET_{EFF} = 75MeV-cm^2/ mg at 125°C.

Table of Contents

1 Overview......2
2 SEE Mechanisms......3
3 Irradiation Facilities and Telemetry......3
4 Test Device and Test Board Information......4
4.1 Qualification Circuits and Boards......4
4.2 Characterization Devices and Test Board Schematics......6
5 Results......8
5.1 SEL Qualification Results......8
5.2 SET Characterization Results: MSU FRIB Linac......12
5.3 Analysis......15
5.4 Weibull Fit......18
6 Summary......20
A MSU Results Appendix......20
B Confidence Interval Calculations......23
C References......25

Trademarks

All trademarks are the property of their respective owners.

Copyright © 2025 Texas Instruments Incorporated

1 Overview

The INA1H94-SP is a radiation-hardened precision unity-gain difference amplifier with a very high input common-mode voltage range. The INA1H94-SP is a single, monolithic device that consists of a precision op amp and an integrated thin-film resistor network. The INA1H94-SP can accurately measure small differential voltages in the presence of common-mode signals up to ±150V. In many applications where galvanic isolation is not required, the INA1H94-SP can replace isolation amplifiers. The excellent 0.0005% typical nonlinearity, high common mode, and 500kHz bandwidth of the INA1H94-SP makes for a compelling sensor readout device. This device runs on a single 4V to 18V supply or dual ±2.V to ±9V supplies.

Table 1-1. Overview Information [(1)]

Description	Device Information
TI Part Number	INA1H94-SP
MLS Number	INA1H94HKX/EM
DLA SMD	5962R2121201VXC
Device Function	INA1H94-SP Radiation-Hardened, High Common-Mode Voltage Difference Amplifier
Fab Technology	BICMOS
Fab Process	BICOM-3XHV
Exposure Facilities	Single Event Effects Facility, Facility for Rare Isotope Beams, Michigan State University
Heavy Ion Fluence per Run	1×10^7 ions/cm^2
Irradiation Temperature	125°C (for SEL testing)

(1) TI may provide technical, applications or design advice, quality characterization, and reliability data or service, providing these items shall not expand or otherwise affect TI's warranties as set forth in the Texas Instruments Incorporated Standard Terms and Conditions of Sale for Semiconductor Products and no obligation or liability shall arise from Semiconductor Products and no obligation or liability shall arise from TI's provision of such items.

Copyright © 2025 Texas Instruments Incorporated

2 SEE Mechanisms

The primary single-event effect (SEE) of interest in the INA1H94-SP is single-event latch-up (SEL). From a risk and potential impact point-of-view, the occurrence of an SEL is possibly the most destructive SEE event and the biggest concern for space applications. A BICMOS process node was used for the INA1H94-SP, though the device is primarily bipolar. CMOS circuitry often introduces a potential for SEL susceptibility. SEL can occur if excess current injection caused by the passage of an energetic ion is high enough to trigger the formation of a parasitic cross-coupled PNP and NPN bipolar structure (formed between the p-sub and n-well and n+ and p+ contacts). The parasitic bipolar structure initiated by a single-event creates a high-conductance path (inducing a steady-state current that is typically orders of magnitude higher than the normal operating current) between power and ground that persists (is *latched*) until the power is removed or until the device is destroyed by the high-current state.

The INA1H94-SP is specified as SEL-free to a surface LET_{EFF} of 75MeV-cm^2/ mg, at a fluence of 10^7 ions / cm^2 and a chip temperature of 125°C. The INA1H94-SP was shown in characterization to exhibit no SEL with heavy ions up to a surface LET_{EFF} of 75MeV-cm^2/ mg, at a fluence of 10^7 ions / cm^2 and a chip temperature of 125°C.

3 Irradiation Facilities and Telemetry

For SEL qualification and SET characterization testing, heavy ion species were provided and delivered by the MSU Facility for Rare Isotope Beams[(4)] (FRIB) using a linear particle accelerator ion source. Ion beams were delivered with high uniformity over a 17mm × 18mm area for the in-air station. A current-based measurement is performed on the collimating slits, which intercept 90-95% of the total beam, and this measurement is cross-calibrated against Faraday cup readings. These measurements are real-time continuous and establish dosimetry and integrated fluence. In-vacuum and in-air scintillating viewers are used for measurement of the beam size and distribution. An ion flux of 10^5 ions / s-cm^2 was used to provide heavy ion fluences to 10^7 ions / cm^2 for most runs. Ion flux was reduced to 10^4 ions / s-cm^2 for some runs, to show SEL immunity at multiple flux rates and to explore the effect of flux rate on transient event counts.

For SET testing, the FRIB "degrader wheel" was employed to adjust the ion energy. The wheel is positioned between the beam "window" or output, and the device under test. The wheel features multiple slots where a foil degrading element of known thicknesses can be loaded. When the wheel is rotated to an "open" slot, only the 70mm air gap and the copper foil in the LINAC path serve to degrade the ion energy. When the wheel is remotely rotated to a slot with a given aluminum degrading foil thickness, the ions pass through the aluminum foil as well, and are slowed accordingly. This decreases the effective ion range in silicon, but increases the effective Linear Energy Transfer (LET_{eff}) in MeV-cm^2/mg, effectively shifting *along* the Bragg curve. Use of the degrader wheel allows multiple LET_{eff} values to be achieved per beam species and LINAC energy level, reducing the switching time and improving testing throughput.

Table 3-1. Effective Surface LET for Various Beam Species and Degrader Thicknesses

Beam species	LINAC energy (MEV/u)	Nominal Cu foil width (µm)	Airgap (mm)	Al degrader thickness (µm)	LET_{eff} at DUT (MeV-cm^2/mg)	Range in Si at DUT (µm)	Notes
^{169}Tm	20.3	5	70	0	75.0	90	No degrader foil used
^{129}Xe	25	5	70	50.8	60.4	86	Comparable to 20MeV/u Xe beam
^{129}Xe	25	5	70	0	50.5	144	No degrader foil used
^{86}Kr	25	5	70	127	35.7	71	Comparable to 17MeV/u Kr beam
^{86}Kr	25	5	70	76.2	29.0	128	Comparable to 20MeV/u Kr beam
^{86}Kr	25	5	70	0	23.1	217	No degrader foil used
^{40}Ar	30	10	70	381	10.8	101	Comparable to 15MeV/u Ar beam

Copyright © 2025 Texas Instruments Incorporated

Table 3-1. Effective Surface LET for Various Beam Species and Degrader Thicknesses (continued)

Beam species	LINAC energy (MEV/u)	Nominal Cu foil width (µm)	Airgap (mm)	Al degrader thickness (µm)	LET_{eff} at DUT (MeV-cm^2/mg)	Range in Si at DUT (µm)	Notes
^{40}Ar	30	10	70	279.4	7.83	216	Comparable to 20MeV/u Ar beam
^{40}Ar	30	10	70	152.4	6.23	361	Comparable to 25MeV/u Ar beam
^{40}Ar	30	10	70	0	5.25	534	No degrader foil used
^{16}O	20	10	70	0	1.49	471	No degrader foil used

4 Test Device and Test Board Information

The INA1H94-SP is packaged in an 8-pin CFP package. Figure 4-1 shows the pinout diagram. The package lid was removed to reveal the die face for all heavy ion testing.

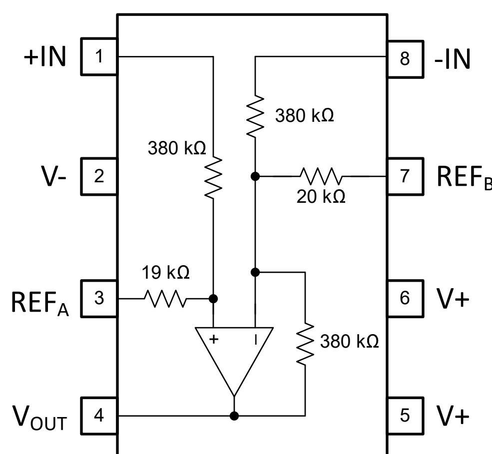

Figure 4-1. INA1H94-SP Pinout Diagram

Each device under test, or DUT, used for single-event effect qualification and characterization was sourced from the same wafer fab and assembly lot, which was used for all INA1H94-SP qualification studies. Across the SEL, SET, and absolute-maximum supply extended SEL characterization tests performed, a total of 12 different devices were evaluated. Some lookahead testing was also performed on units from different wafer fab and assembly lots, with no significant differences observed in the test results.

4.1 Qualification Circuits and Boards

The INA1H94-SP was biased in a variety of different conditions for SEE testing, at both the recommended minimum and recommended maximum supply voltages. Midsupply or GND was used for both REF_A and REF_B. Current was monitored over time for both V+ and V-.

Copyright © 2025 Texas Instruments Incorporated

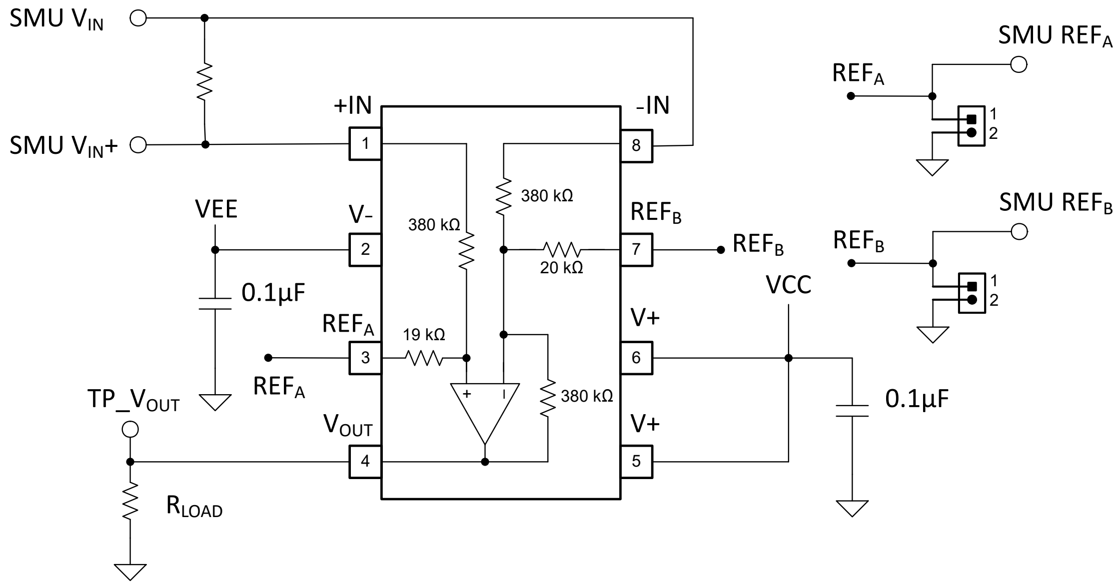

Figure 4-2. INA1H94-SP SEE Qualification Bias Diagram

Input and supply voltages were provided by SMU PXI cards, connected with banana cables. The board used for testing incorporated jumpers to allow testing with high V_{CM} and 0V V_{DIFF}; low V_{CM} and high V_{DIFF}; and high V_{CM} and constant V_{DIFF}. For all testing, the device outputs were monitored using oscilloscope PXI cards, connected with BNC cables. 100Ω of series isolation resistance was used on each output channel to drive the cable capacitance. A 2kΩ output load to midsupply was present for all DUTs.

An example of three decapped units mounted on a characterization board is shown in Figure 4-3. Note that for SET testing, devices were powered in parallel and the test facility "stage" or backplane was moved between runs to target different DUTs. For SEL testing, only one device was connected at a time.

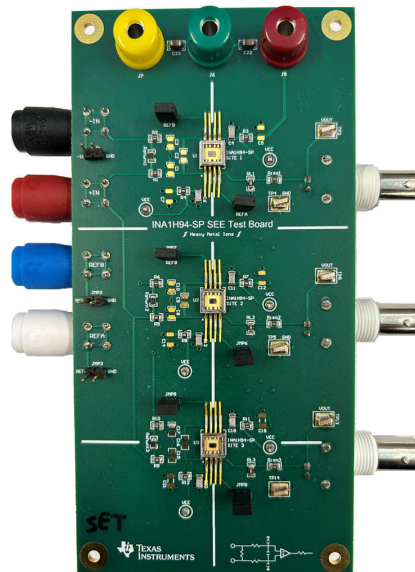

Figure 4-3. Characterization Board

Additional correlation testing was performed on three units, each mounted on a simplified coupon board, using the device absolute maximum supply voltage (24V). Devices were exposed to a total fluence of 5×10^7 ions / cm^2 (60krad of accumulated HDR TID), 2×10^7 ions / cm^2 (24krad of accumulated HDR TID), and 1×10^7 ions / cm^2 (12krad of accumulated HDR TID) respectively without any failures observed. This suggests the device has significant margin at the device recommended maximum operating voltage of 18V.

Copyright © 2025 Texas Instruments Incorporated

4.2 Characterization Devices and Test Board Schematics

Heavy ions were used to irradiate the devices. A nominal flux of 1 × 10^5 ions / s-cm^2 was used for SEL characterization, at 125°C die temperature. Nominal flux of 1 × 10^5 ions / s-cm^2 was used for SET characterization, at ambient temperature.

For SEE characterization, the INA1H94-SP was biased with bipolar split supplies. The circuit was connected as shown on Figure 4-4. Different supply voltages, input common-mode voltages and differential voltage conditions were tested.

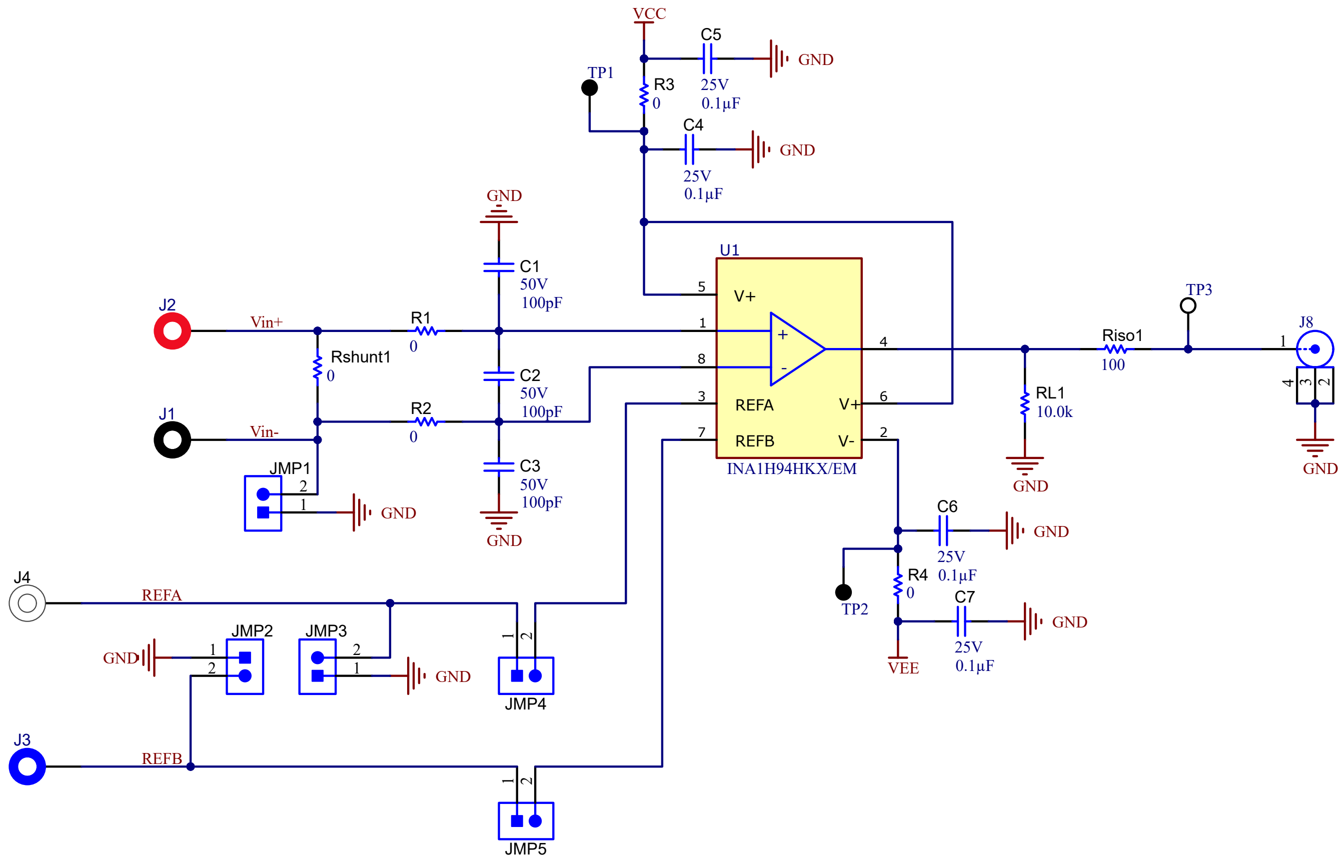

Figure 4-4. SEE Characterization Board Schematic (Site 1 Only)

Input and supply voltages were provided by SMU PXI cards, connected with banana cables. A common input signal was applied to all channels. Figure 4-5 shows the decoupling capacitance scheme used on each board. Current was monitored over time for both V+ and V-. For SET testing, the device outputs were monitored using oscilloscope PXI cards, connected with BNC cables. 100Ω of series isolation resistance was used on the output channel to drive the cable capacitance.

Copyright © 2025 Texas Instruments Incorporated

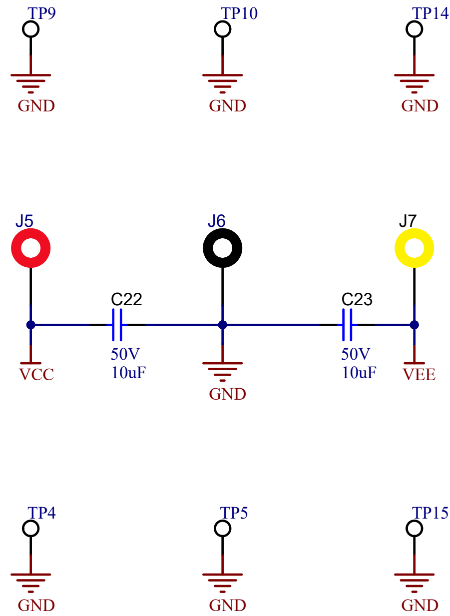

Figure 4-5. Characterization Board Voltage Supply Connections

Copyright © 2025 Texas Instruments Incorporated

5 Results

5.1 SEL Qualification Results

During SEL qualification, the device was heated using forced hot air, maintaining an IC temperature at 125°C. The temperature was monitored using a thermal camera. The species used for the SEL testing was a thulium (^{169}Tm) ion with an angle-of-incidence of 0° and an air gap of 70mm, for an LET_{EFF} = 75MeV-cm^2/mg. A nominal flux of 10^5 ions / s-cm^2 and fluence of 10^7 ions / cm^2 were targeted for each run. A total of five different DUTs were used for this testing, together experiencing a cumulative total fluence of approximately 30 × 10^7 ions / cm^2 with no failures observed.

An exhaustive summary of the conditions for the 3 SEL test runs performed is provided in Table 5-1. The run numbers listed are the actual run numbers from the testing session, and the flux, fluence, and dose in silicon for each run are pulled from the test session log provided by the MSU FRIB. Note that some runs, such as 13-15, from the session are excluded from the table because these runs were used to test other non-INA1H94-SP devices. Figure 5-2 and related figures show example plots of the supply currents versus time.

Table 5-1. INA1H94-SP SEL Testing Summary, ^{169}Tm Ion, 125°C Die Temperature

Run #	DUT	V+ Supply (V)	V- Supply (V)	V_{CM}| V_{DIFF}	Input (V)	Mean Flux (ions × cm^2/mg)	Fluence (Number ions)	Dose in Silicon (rad)
1	SEL1_1	2.5	-2.5	V_{DIFF}	1	$1×10^4$	$1×10^7$	12000
2	SEL1_1	9	-9	V_{DIFF}	5	$1×10^4$	$9.24×10^6$	11085
3	SEL1_1	9	-9	V_{DIFF}	5	$1×10^5$	$1×10^7$	12000
4	SEL1_1	2.5	-2.5	V_{DIFF}	1	$1×10^5$	$1×10^7$	12000
5	SEL2_1	2.5	-2.5	V_{CM}	10	$1×10^5$	$1×10^7$	12000
6	SEL2_1	2.5	-2.5	V_{CM}	-22.5	$1×10^5$	$1×10^7$	12000
7	SEL2_1	2.5	-2.5	V_{CM}	22.5	$1×10^5$	$1×10^7$	12000
8	SEL2_1	9	-9	V_{CM}	10	$1×10^5$	$1×10^7$	12000
9	SEL2_1	9	-9	V_{CM}	150	$1×10^5$	$1×10^7$	12000
10	SEL2_1	9	-9	V_{CM}	-150	$1×10^5$	$1×10^7$	12000
11	SEL2_1	12	-12	V_{CM}	150	$1×10^5$	$1×10^7$	12000
12	SEL2_1	12	-12	V_{CM}	-150	$1×10^5$	$1×10^7$	12000
16	SEL1_2	2.5	-2.5	V_{CM}	22.5	$1×10^5$	$1×10^7$	12000
17	SEL1_2	2.5	-2.5	V_{CM}	-22.5	$1×10^5$	$1×10^7$	12000
18	SEL1_2	9	-9	V_{CM}	-150	$1×10^5$	$1×10^7$	12000
19	SEL1_2	9	-9	V_{CM}	150	$1×10^5$	$1×10^7$	12000
20	SEL1_2	9	-9	V_{DIFF}	-7.5	$1×10^5$	$1×10^7$	12000
21	SEL1_2	9	-9	V_{DIFF}	7.5	$1×10^5$	$1×10^7$	12000
22	SEL1_2	2.5	-2.5	V_{DIFF}	1	$1×10^5$	$1×10^7$	12000
23	SEL2_2	2.5	-2.5	V_{CM}	-22.5	$1×10^5$	$1×10^7$	12000
24	SEL2_2	2.5	-2.5	V_{CM}	22.5	$1×10^5$	$1×10^7$	12000
25	SEL2_2	9	-9	V_{CM}	150	$1×10^5$	$1×10^7$	12000
26	SEL2_2	9	-9	V_{CM}	-150	$1×10^5$	$1×10^7$	12000
27	SEL2_2	9	-9	V_{DIFF}	-7.5	$1×10^5$	$1×10^7$	12000
28	SEL2_2	9	-9	V_{DIFF}	7.5	$1×10^5$	$1×10^7$	12000
29	SEL2_2	2.5	-2.5	V_{DIFF}	1	$1×10^5$	$1×10^7$	12000
32	SEL2_3	2.5	-2.5	V_{CM} | V_{DIFF}	22.5 | 1V	$1×10^5$	$1×10^7$	12000
33	SEL2_3	2.5	-2.5	V_{CM} | V_{DIFF}	-22.5 | -1V	$1×10^5$	$1×10^7$	12000
34	SEL2_3	9	-9	V_{CM} | V_{DIFF}	-150 | 7.5V	$1×10^5$	$1×10^7$	12000
35	SEL2_3	9	-9	V_{CM} | V_{DIFF}	150 | -7.5V	$1×10^5$	$1×10^7$	12000

Copyright © 2025 Texas Instruments Incorporated

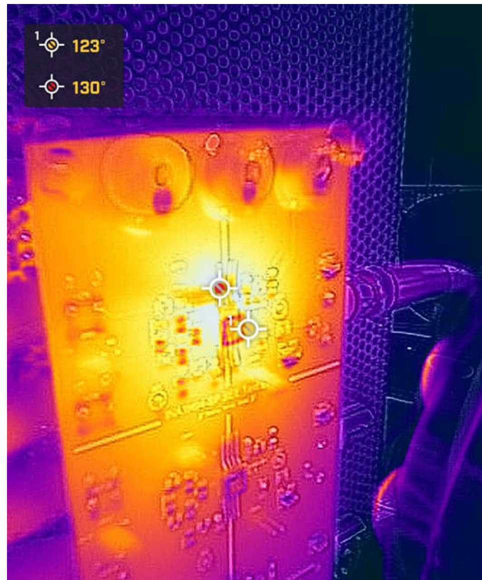

Figure 5-1. Thermal Image During Set Up

No SEL events were observed, which indicates that the INA1H94-SP is SEL-immune at LET_{EFF} = 75MeV-cm^2/mg and T = 125°C.

$\sigma SEL \leq 1.84 \times 10^{-7}$ cm^2 for LET_{EFF} = 75MeV-cm^2/ mg and T = 125°C.

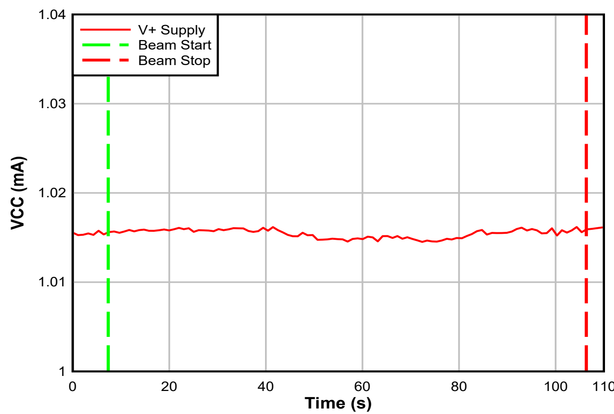

Figure 5-2. Current Versus Time (I Versus t) Data for V+ Current During SEL Run 4

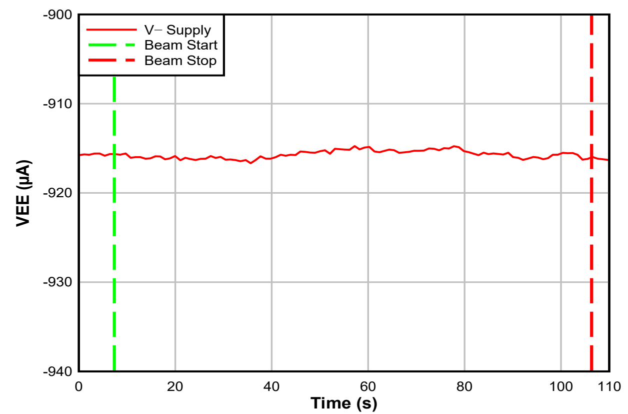

Figure 5-3. Current Versus Time (I Versus t) Data for V- Current During SEL Run 4

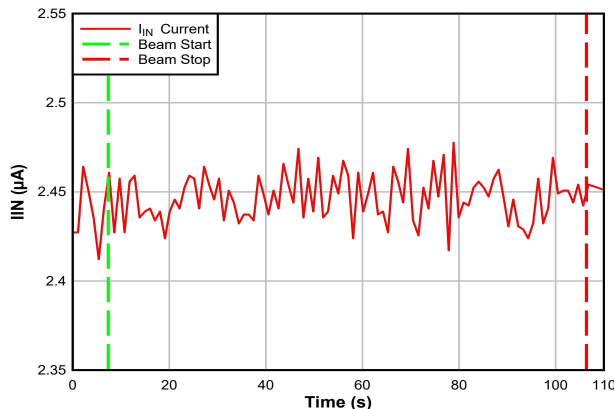

Figure 5-4. Current Versus Time (I Versus t) Data for I_{IN} Current During SEL Run 4

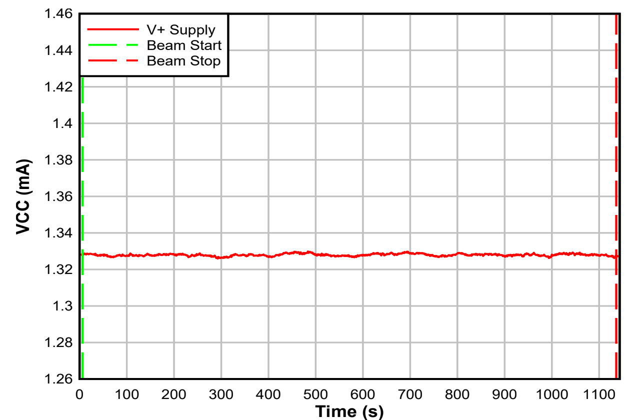

Figure 5-5. Current Versus Time (I Versus t) Data for V+ Current During SEL Run 2

Copyright © 2025 Texas Instruments Incorporated

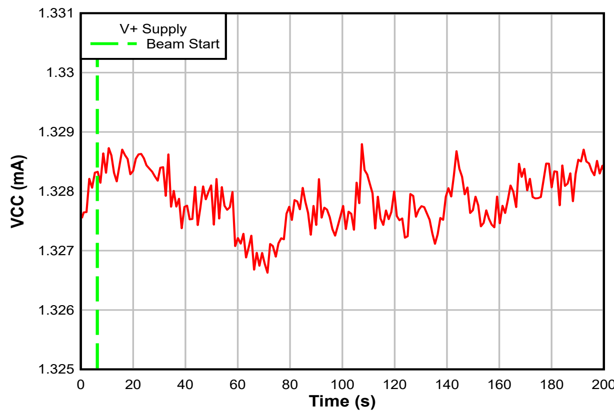

Figure 5-6. Current Versus Time (I Versus t) Data for V+ Current During SEL Run 2 (Zoom In)

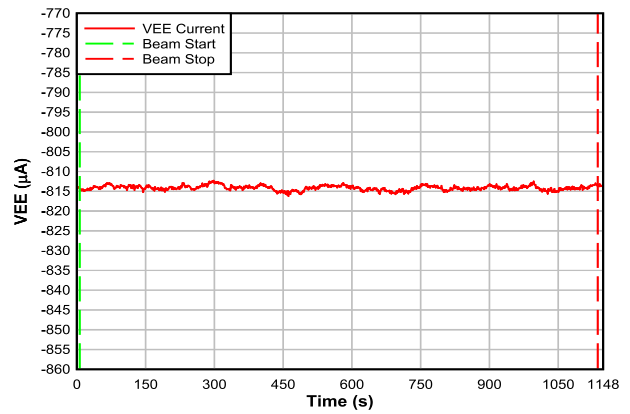

Figure 5-7. Current Versus Time (I Versus t) Data for V- Current During SEL Run 2

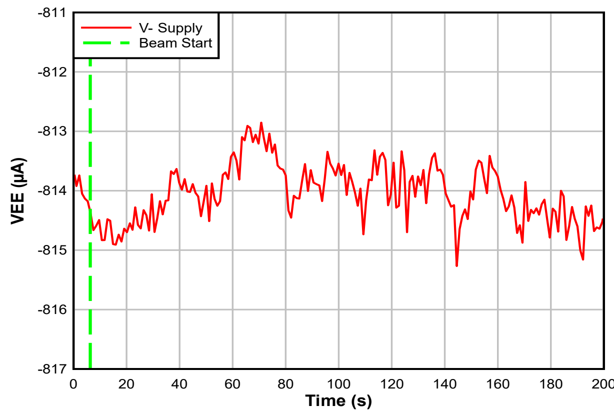

Figure 5-8. Current Versus Time (I Versus t) Data for V- Current During SEL Run 2 (Zoom In)

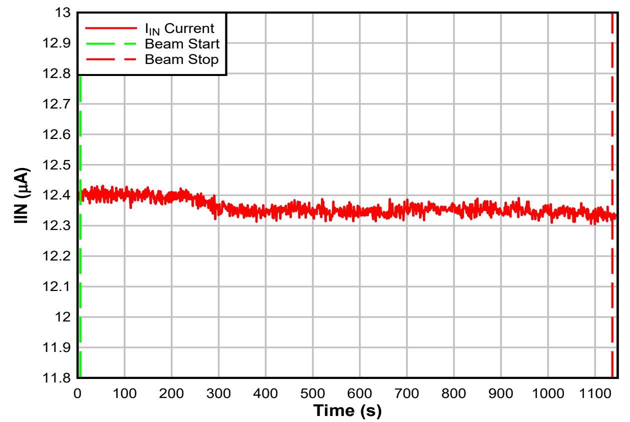

Figure 5-9. Current Versus Time (I Versus t) Data for I_{IN} Current During SEL Run 2

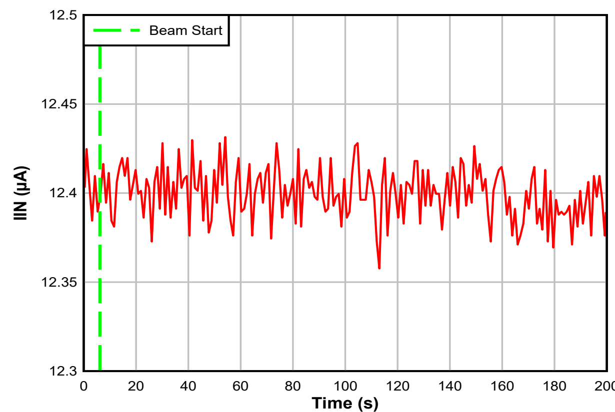

Figure 5-10. Current Versus Time (I Versus t) Data for I_{IN} Current During SEL Run 2 (Zoom In)

Copyright © 2025 Texas Instruments Incorporated

An additional SMU SEL session was performed with 3 fresh devices. A summary of the conditions in test runs performed is provided in Table 5-2. On this session, devices were tested up to the absolute maximum supply of 24V without any failures observed.

Table 5-2. Second Session INA1H94-SP SEL Test Summary, ^{169}Tm Ion, 125°C Die Temperature

Run #	DUT	V+ Supply (V)	V- Supply (V)	V_{CM}| V_{DIFF}	Input (V)	Mean Flux (ions × cm^2/mg)	Fluence (Number ions)	Dose in Silicon (rad)
24	C0	9	-9	V_{DIFF}	2	1×10^5	1×10^7	11957
25	C0	12	-12	V_{DIFF}	2	1×10^5	1×10^7	11957
26	C0	12	-12	V_{DIFF}	2	1×10^5	2×10^7	23904
27	C0	12	-12	V_{DIFF}	2	1×10^5	1×10^7	11957
28	C0	12	-12	V_{DIFF}	2	1×10^5	1×10^7	11957
29	C0	12	-12	V_{DIFF}	2	1×10^5	1×10^7	11957
30	C0	12	-12	V_{DIFF}	2	1×10^5	1×10^7	11957
31	C1	9	-9	V_{DIFF}	2	1×10^5	3×10^7	36484
32	C1	12	-12	V_{DIFF}	2	1×10^5	2×10^7	23904
33	C2	12	-12	V_{DIFF}	2	1×10^5	2×10^7	23904
34	C2	12	-12	V_{DIFF}	2	1×10^5	3×10^7	36484
35	C2	12	-12	V_{DIFF}	2	1×10^5	5×10^7	59978

Copyright © 2025 Texas Instruments Incorporated

5.2 SET Characterization Results: MSU FRIB Linac

Three fresh DUTs were used for SET characterization. The conditions for each run are summarized on Table 5-3 below.

The device was tested at maximum specified supply voltage range of ±9V (or 18V total supply) and input common mode voltage (V_{CM}) of ±150V with a fixed input differential voltage V_{DIFF}. he REFA and REFB pins were biased at mid-supply (0V). The device output channel was loaded with a 2kΩ resistance to GND (midsupply). Tests were repeated at the lower specified supply voltage range of ±2.5V (or 5V total supply) with V_{CM} =±22.5V.

The oscilloscopes were set to a *window* trigger mode that captured any events where the output shifted by ±100mV or more.

The devices were exposed to LET levels varying from 75MeV-cm^2 / mg to 1.5MeV-cm^2 / mg. An ambient temperature of approximately 20°C was recorded in the facility at the time of these tests. See Appendix A for additional data, such as histograms.

Runs 39, 41, 117, 119 from the session are excluded on the table. These runs were interruped due to set up adjustments. However, the same DUT test conditions were repeated in the following run.

Table 5-3. SMU SET Characterization Run Summary

Run Number	DUT	Supply (V)	V_{DIFF} (V)	V_{CM} (V)	Ion	LETeff (MeV-cm^2/mg)	Flux (ions/s-cm^2)	Fluence (ions/cm^2)	Total Ionizing Dose (rad)	Events
36	SET_1	±2.5	0.544	22.5	^{169}Tm	75	1×10^5	1×10^7	12000	13255
37	SET_1	±2.5	-0.544	-22.5	^{169}Tm	75	1×10^5	1×10^7	12000	13662
38	SET_1	±9	3.614	150	^{169}Tm	75	1×10^5	1×10^7	1E7	14983
40	SET_1	±9	-3.614	-150	^{169}Tm	75	1×10^5	1×10^7	12000	15611
42	SET_2	±2.5	0.544	22.5	^{169}Tm	75	1×10^5	1×10^7	12000	13799
43	SET_2	±2.5	-0.544	-22.5	^{169}Tm	75	1×10^5	1×10^7	12000	14295
44	SET_2	±9	3.614	150	^{169}Tm	75	1×10^5	1×10^7	12000	15779
45	SET_2	±9	-3.614	-150	^{169}Tm	75	1×10^5	1×10^7	12000	16414
46	SET_3	±2.5	0.544	22.5	^{169}Tm	75	1×10^5	1×10^7	12000	14099
47	SET_3	±2.5	-0.544	-22.5	^{169}Tm	75	1×10^5	1×10^7	12000	14584
48	SET_3	±9	-3.614	-150	^{169}Tm	75	1×10^5	1×10^7	12000	16979
49	SET_3	±9	3.614	150	^{169}Tm	75	1×10^5	1×10^7	12000	15732
50	SET_1	±2.5	0.544	22.5	^{129}Xe	60.3	1×10^5	1×10^7	9650	12138
51	SET_1	±2.5	-0.544	-22.5	^{129}Xe	60.3	1×10^5	1×10^7	9650	12226
52	SET_1	±9	3.614	150	^{129}Xe	60.3	1×10^5	1×10^7	9650	12054
53	SET_1	±9	-3.614	-150	^{129}Xe	60.3	1×10^5	1×10^7	9650	13101
54	SET_1	±9	-3.614	-150	^{129}Xe	50.4	1×10^5	1×10^7	8000	13441
55	SET_1	±9	3.614	150	^{129}Xe	50.4	1×10^5	1×10^7	8000	12611
56	SET_1	±2.5	-0.544	-22.5	^{129}Xe	50.4	1×10^5	1×10^7	8000	13174
57	SET_1	±2.5	0.544	22.5	^{129}Xe	50.4	1×10^5	1×10^7	8000	12939
58	SET_2	±2.5	0.544	22.5	^{129}Xe	60.3	1×10^5	1×10^7	9650	13791
59	SET_2	±9	3.614	150	^{129}Xe	60.3	1×10^5	1×10^7	9650	14534
60	SET_2	±9	3.614	150	^{129}Xe	50.4	1×10^5	1×10^7	8000	14589
61	SET_2	±2.5	0.544	22.5	^{129}Xe	50.4	1×10^5	1×10^7	8000	13661
62	SET_3	±2.5	0.544	22.5	^{129}Xe	60.3	1×10^5	1×10^7	9650	14342
63	SET_3	±9	3.614	150	^{129}Xe	60.3	1×10^5	1×10^7	9650	15482
64	SET_3	±9	3.614	150	^{129}Xe	50.4	1×10^5	1×10^7	8000	15265
65	SET_3	±2.5	0.544	22.5	^{129}Xe	50.4	1×10^5	1×10^7	8000	14191
66	SET_3	±2.5	0.544	22.5	^{86}Kr	35.6	1×10^5	1×10^5	5700	9239

Copyright © 2025 Texas Instruments Incorporated

Table 5-3. SMU SET Characterization Run Summary (continued)

Run Number	DUT	Supply (V)	V_{DIFF} (V)	V_{CM} (V)	Ion	LETeff (MeV-cm²/mg)	Flux (ions/s-cm²)	Fluence (ions/cm²)	Total Ionizing Dose (rad)	Events
67	SET_3	±9	3.614	150	^{86}Kr	35.6	$1{\times}10^5$	$1{\times}10^7$	5700	10087
68	SET_3	±9	3.614	150	^{86}Kr	28.9	$1{\times}10^5$	$1{\times}10^7$	4600	9897
69	SET_3	±2.5	0.544	22.5	^{86}Kr	28.9	$1{\times}10^5$	$1{\times}10^7$	4600	9228
70	SET_3	±2.5	0.544	22.5	^{86}Kr	23.1	$1{\times}10^5$	$1{\times}10^7$	3700	9142
71	SET_3	±9	3.614	150	^{86}Kr	23.1	$1{\times}10^5$	$1{\times}10^7$	3700	9574
72	SET_2	±9	3.614	150	^{86}Kr	35.6	$1{\times}10^5$	$1{\times}10^7$	5700	9847
73	SET_2	±2.5	0.544	22.5	^{86}Kr	35.6	$1{\times}10^5$	$1{\times}10^7$	5700	9423
74	SET_2	±2.5	0.544	22.5	^{86}Kr	28.9	$1{\times}10^5$	$1{\times}10^7$	4600	9533
75	SET_2	±9	3.614	150	^{86}Kr	28.9	$1{\times}10^5$	$1{\times}10^7$	4600	9894
76	SET_2	±9	3.614	150	^{86}Kr	23.1	$1{\times}10^5$	$1{\times}10^7$	3700	9561
77	SET_2	±2.5	0.544	22.5	^{86}Kr	23.1	$1{\times}10^5$	1.4E6	456	1110
78	SET_2	±2.5	0.544	22.5	^{86}Kr	23.1	$1{\times}10^5$	$1{\times}10^7$	3700	9269
79	SET_1	±2.5	0.544	22.5	^{86}Kr	35.6	$1{\times}10^5$	$1{\times}10^7$	5700	9247
80	SET_1	±2.5	-0.544	-22.5	^{86}Kr	35.6	$1{\times}10^5$	$1{\times}10^7$	5700	9524
81	SET_1	±9	3.614	150	^{86}Kr	35.6	$1{\times}10^5$	$1{\times}10^7$	5700	9755
82	SET_1	±9	-3.614	-150	^{86}Kr	35.6	$1{\times}10^5$	$1{\times}10^7$	5700	10095
83	SET_1	±9	-3.614	-150	^{86}Kr	28.9	$1{\times}10^5$	$1{\times}10^7$	4600	10129
84	SET_1	±9	3.614	150	^{86}Kr	28.9	$1{\times}10^5$	$1{\times}10^7$	4600	9449
85	SET_1	±2.5	0.544	22.5	^{86}Kr	28.9	$1{\times}10^5$	$1{\times}10^7$	4600	9164
86	SET_1	±2.5	-0.544	-22.5	^{86}Kr	28.9	$1{\times}10^5$	$1{\times}10^7$	4600	9347
87	SET_1	±2.5	-0.544	-22.5	^{86}Kr	23.1	$1{\times}10^5$	$1{\times}10^7$	3700	9052
88	SET_1	±2.5	0.544	22.5	^{86}Kr	23.1	$1{\times}10^5$	$1{\times}10^7$	3700	9058
89	SET_1	9	3.614	150	^{86}Kr	23.1	$1{\times}10^5$	$1{\times}10^7$	3700	9189
90	SET_1	±9	-3.614	-150	^{86}Kr	23.1	$1{\times}10^5$	$1{\times}10^7$	3700	9841
91	SET_3	±9	3.614	150	^{40}Ar	10.3	$1{\times}10^5$	$1{\times}10^7$	1650	5923
92	SET_3	±2.5	0.544	22.5	^{40}Ar	10.3	$1{\times}10^5$	$1{\times}10^7$	1650	5358
93	SET_3	±2.5	0.544	22.5	^{40}Ar	6.9	$1{\times}10^5$	$1{\times}10^7$	1100	5028
94	SET_3	±9	3.614	150	^{40}Ar	6.9	$1{\times}10^5$	$1{\times}10^7$	1100	5188
95	SET_3	±9	3.614	150	^{40}Ar	5.3	$1{\times}10^5$	$1{\times}10^7$	840	5104
96	SET_3	±2.5	0.544	22.5	^{40}Ar	5.3	$1{\times}10^5$	$1{\times}10^7$	840	5108
97	SET_2	±2.5	0.544	22.5	^{40}Ar	10.3	$1{\times}10^5$	$1{\times}10^7$	1650	5244
98	SET_2	±9	3.614	150	^{40}Ar	10.3	$1{\times}10^5$	$1{\times}10^7$	1650	5435
99	SET_2	±9	3.614	150	^{40}Ar	6.9	$1{\times}10^5$	$1{\times}10^7$	1100	5204
100	SET_2	±2.5	0.544	22.5	^{40}Ar	6.9	$1{\times}10^5$	$1{\times}10^7$	1100	5316
101	SET_2	±2.5	0.544	22.5	^{40}Ar	5.3	$1{\times}10^5$	$1{\times}10^7$	840	5172
102	SET_2	±9	3.614	150	^{40}Ar	5.3	$1{\times}10^5$	$1{\times}10^7$	840	5034
103	SET_3	±9	3.614	150	^{40}Ar	10.3	$1{\times}10^5$	$1{\times}10^7$	1650	4757
104	SET_3	±9	-3.614	-150	^{40}Ar	10.3	$1{\times}10^5$	$1{\times}10^7$	1650	4746
105	SET_3	±2.5	0.544	22.5	^{40}Ar	10.3	$1{\times}10^5$	$1{\times}10^7$	1650	4854
106	SET_3	±2.5	-0.544	-22.5	^{40}Ar	10.3	$1{\times}10^5$	$1{\times}10^7$	1650	4853
107	SET_3	±2.5	-0.544	-22.5	^{40}Ar	6.9	$1{\times}10^5$	$1{\times}10^7$	1100	4939
108	SET_3	±2.5	0.544	22.5	^{40}Ar	6.9	$1{\times}10^5$	$1{\times}10^7$	1100	4826
109	SET_3	±9	3.614	150	^{40}Ar	6.9	$1{\times}10^5$	$1{\times}10^7$	1100	4762
110	SET_3	±9	-3.614	-150	^{40}Ar	6.9	$1{\times}10^5$	$1{\times}10^7$	1100	4892

Copyright © 2025 Texas Instruments Incorporated

Table 5-3. SMU SET Characterization Run Summary (continued)

Run Number	DUT	Supply (V)	V_{DIFF} (V)	V_{CM} (V)	Ion	LETeff (MeV-cm^2/mg)	Flux (ions/s-cm^2)	Fluence (ions/cm^2)	Total Ionizing Dose (rad)	Events
111	SET_3	±9	-3.614	-150	^{40}Ar	5.3	1×10^5	1×10^7	840	4737
112	SET_3	±9	3.614	150	^{40}Ar	5.3	1×10^5	1×10^7	840	4628
113	SET_3	±2.5	0.544	22.5	^{40}Ar	5.3	1×10^5	1×10^7	840	4581
114	SET_3	±2.5	-0.544	-22.5	^{40}Ar	5.3	1×10^5	1×10^7	840	4624
115	SET_1	±2.5	-0.544	-22.5	^{16}O	1.5	1×10^5	1×10^7	240	2828
116	SET_1	±2.5	0.544	22.5	^{16}O	1.5	1×10^5	1×10^7	240	2795
118	SET_1	±9	3.614	150	^{16}O	1.5	1×10^5	1×10^7	240	2553
120	SET_1	±9	-3.614	-150	^{16}O	1.5	1×10^5	1×10^7	240	2553
121	SET_2	±9	3.614	150	^{16}O	1.5	1×10^5	4×10^6	240	2426
122	SET_2	±2.5	0.544	22.5	^{16}O	1.5	1×10^5	1×10^7	240	2999
123	SET_3	±9	3.614	150	^{16}O	1.5	1×10^5	1×10^7	240	2637
124	SET_3	±2.5	0.544	22.5	^{16}O	1.5	1×10^5	1×10^7	240	2739

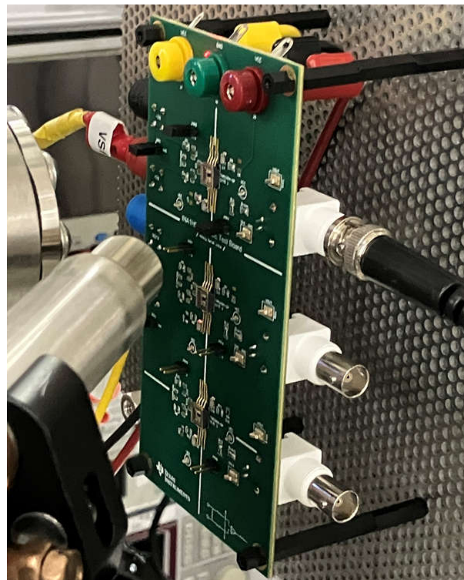

Figure 5-11. Device Under Test Lined Up With the Beam

Copyright © 2025 Texas Instruments Incorporated

5.3 Analysis

Information in this section describes general characteristics of the SET response characteristics of the device, and may not be accurate for all use cases or conditions. In-circuit results vary according to application specifics. TI's customers are responsible for determination of components for their purposes, and validating and testing design implementation to confirm system functionality.

The data suggest the rate at which the INA1H94-SP exhibits SET events, and the magnitude of those events, is a function of several factors. These include supply voltage, input common-mode voltage (V_{CM}), differential input voltage (VDIFF) beam flux, ion energy, and temperature.

Generally, when the INA1H94-SP experiences an SET, the device output presents sudden *spikes* and are usually resolved within 10µs of the trigger event. Events where the output shifted by more than ±100mV were recorded by the oscilloscope cards. A small percentage of these captures show measurable undershoot or overshoot behavior after the initial spike as the output settles. Table 5-4 shows notable oscilloscope captures.

Note that the INA1H94-SP also experiences transient events of less than 100mV. As a result, this study focuses on only events more than 100mV in magnitude. Testing at MSU has shown that the beam area is an electrically noisy environment, which can lead to false trigger events. As a result, this study focuses on only events more than 100mV in magnitude. Implementing filters on the device to reject noise can lead to reductions in SET count or impact the magnitude of those events.

Device DUT-SET1 was evaluated with ion energy in *descending* order, from 75MeV-cm^2 / mg to 1.4MeV-cm^2 / mg with the exception of ion energy levels of 10.3MeV-cm^2 / mg, 6.9MeV-cm^2 / mg and 5.3MeV-cm^2 / mg. This device was evaluated with both positive and negative polarity V_{CM} and V_{DIFF} input voltages.

Devices DUT-SET2 and DUT-SET3 were also evaluated at the same energy levels, with the addition of levels of 6.9MeV-cm^2 / mg and 5.3MeV-cm^2 / mg.

Table 5-4. Sum of Event Counts Per Device

LET (MeV-cm^2 /mg)	Parameter	DUT-SET1		DUT-SET2		DUT-SET3	
		Vs = 5V	Vs = 18V	Vs = 5V	Vs = 18V	Vs = 5V	Vs = 18V
75	Events	29273	28238	30709	29578	31563	29831
	Fluence (Ions/cm^2)	2×10^7	2×10^7	2×10^7	2×10^7	2×10^7	2×10^7
	Cross Section (cm^2)	1.46×10^{-3}	1.41×10^{-3}	1.54×10^{-3}	1.48×10^{-3}	1.58×10^{-3}	1.49×10^{-3}
60.3	Events	25327	24192	13791	14534	14342	15482
	Fluence (Ions/cm^2)	2×10^7	2×10^7	1×10^7	1×10^7	1×10^7	1×10^7
	Cross Section (cm^2)	1.27×10^{-3}	1.21×10^{-3}	1.38×10^{-3}	1.45×10^{-3}	1.43×10^{-3}	1.55×10^{-3}
50.4	Events	26615	25550	13661	14589	14191	15265
	Fluence (Ions/cm^2)	2×10^7	2×10^7	1×10^7	1×10^7	1×10^7	1×10^7
	Cross Section (cm^2)	1.33×10^{-3}	1.28×10^{-3}	1.37×10^{-3}	1.46×10^{-3}	1.42×10^{-3}	1.53×10^{-3}
35.6	Events	19619	19002	9423	9847	9239	10087
	Fluence (Ions/cm^2)	2×10^7	2×10^7	1×10^7	1×10^7	1×10^7	2×10^7
	Cross Section (cm^2)	9.81×10^{-4}	9.50×10^{-4}	9.42×10^{-4}	9.85×10^{-4}	9.24×10^{-4}	1.01×10^{-3}
28.9	Events	19476	18613	9533	9894	9228	9897
	Fluence (Ions/cm^2)	2×10^7	2×10^7	1×10^7	1×10^7	1×10^7	1×10^7
	Cross Section (cm^2)	9.74×10^{-4}	9.31×10^{-4}	9.53×10^{-4}	9.89×10^{-4}	9.23×10^{-4}	9.90×10^{-4}
23.1	Events	18893	18247	10379	9561	9142	9574
	Fluence (Ions/cm^2)	2×10^7	2×10^7	1.14×10^7	1×10^7	1×10^7	1×10^7
	Cross Section (cm^2)	9.45×10^{-4}	9.12×10^{-4}	9.10×10^{-4}	9.56×10^{-4}	9.14×10^{-4}	9.57×10^{-4}
10.3	Events	N/A	N/A	5244	5435	9707	9503
	Fluence (Ions/cm^2)			1×10^7	1×10^7	3×10^7	3×10^7
	Cross Section (cm^2)			5.24×10^{-4}	5.44×10^{-4}	4.85×10^{-4}	4.75×10^{-4}

Copyright © 2025 Texas Instruments Incorporated

Table 5-4. Sum of Event Counts Per Device (continued)

LET (MeV-cm^2 /mg)	Parameter	DUT-SET1		DUT-SET2		DUT-SET3	
		Vs = 5V	Vs = 18V	Vs = 5V	Vs = 18V	Vs = 5V	Vs = 18V
6.9	Events	N/A	N/A	5316	5204	14973	14842
	Fluence (Ions/cm^2)			1 x 10^7	1 x 10^7	3 x 10^7	3 x 10^7
	Cross Section (cm^2)			5.32 x 10^{-4}	5.20 x 10^{-4}	4.93 x 10^{-4}	4.95 x 10^{-4}
5.3	Events	N/A	N/A	5172	5034	14313	14469
	Fluence (Ions/cm^2)			1 x 10^7	1 x 10^7	3 x 10^7	3 x 10^7
	Cross Section (cm^2)			5.17x 10^{-4}	5.03 x 10^{-4}	4.77 x 10^{-4}	4.82 x 10^{-4}
1.5	Events	5623	5106	2999	2426	2739	2637
	Fluence (Ions/cm^2)	2 x 10^7	2 x 10^7	1 x 10^7	4 x 10^6	1 x 10^7	1 x 10^7
	Cross Section (cm^2)	2.81 x 10^{-4}	2.55 x 10^{-4}	3.00 x 10^{-4}	6.07 x 10^{-4}	2.74 x 10^{-4}	2.64 x 10^{-4}

The INA1H94-SP susceptibility to SET increases as ion energy level increases. There is also an increase of events as the supply voltage, and magnitude V_{CM} and V_{DIFF} input voltages increase. Input voltages of negative polarity appeared to produce a slightly higher susceptibility to events. In some cases, differences in readings between devices at similar input voltages can be attributed to differences in the oscilloscope cards used, as verified through A↔B site swaps.

Factors such as the time between decap and testing (time the die is exposed to air), annealing time between runs, and simple device-to-device variation can also play a potential role in the differing event counts. Correlating any single factor to the event counts is difficult due to the complexities and practical challenges of the testing.

Table 5-5. Transient Event Summary for 5V Supply

LET (MeV-cm^2 /mg)	Event Count	Mean Transient Duration (µs)	Std. Dev. Transient Duration (µs)	Avg. Pk. Voltage (V)	Std. Dev. Pk. Voltage (V)	Min. Pk Voltage (V)	Max. Pk Voltage (V)	Mean Abs. Pk. Voltage (V)	Std. Dev. peak Voltage (V)
75	28617	0.2290	0.4791	-0.042	0.687	-2.108	1.093	0.483	0.490
60.3	23605	0.2057	0.3854	-0.066	0.715	-2.087	1.032	0.488	0.526
50.4	21431	0.2043	0.3030	-0.060	0.698	-1.979	1.052	0.490	0.501
35.6	14023	0.2050	0.2712	-0.040	0.645	-1.728	1.023	0.465	0.449
28.9	13194	0.2014	0.3378	-0.017	0.573	-2.067	1.022	0.415	0.395
23.1	12168	0.1966	0.2849	-0.011	0.504	-1.405	1.009	0.371	0.342
10.3	6172	0.1812	0.1921	-0.002	0.331	-1.365	0.947	0.291	0.159
6.9	5961	0.1779	0.1701	-0.001	0.222	-1.640	1.018	0.195	0.105
5.3	5520	0.1785	0.1338	-0.003	0.169	-0.948	0.981	0.151	0.076
1.5	2796	0.2287	0.1073	-0.003	0.065	-0.205	0.294	0.064	0.013

Copyright © 2025 Texas Instruments Incorporated

Table 5-6. Transient Event Summary for 18V Supply

LET (MeV-cm^2 /mg)	Event Count	Mean Transient Duration (µs)	Std. Dev. Transient Duration (µs)	Avg. Pk. Voltage (V)	Std. Dev. Pk Voltage (V)	Min Pk. Voltage (V)	Max Pk Voltage (V)	Mean Abs. Pk. Voltage (V)	Std. Dev. Pk. Voltage (V)
75	29634	0.0460	0.0757	0.0623	1.0339	-3.2646	3.5361	0.6736	0.7880
60.3	25118	0.0464	0.0735	0.0211	0.9291	-2.6294	2.8767	0.6040	0.7063
50.4	23691	0.0463	0.0770	0.0138	0.8303	-2.3220	2.4939	0.5510	0.6212
35.6	15128	0.0477	0.0586	0.0051	0.7050	-1.6393	2.7141	0.4976	0.4995
28.9	13921	0.0492	0.0576	-0.0104	0.5956	-1.9142	2.4100	0.4303	0.4120
23.1	12130	0.0484	0.0503	-0.0143	0.5249	-1.2829	1.6225	0.3941	0.3470
10.3	6242	0.0474	0.0445	-0.0019	0.3215	-1.0657	1.0011	0.2801	0.1585
6.9	5963	0.0488	0.0435	-0.0021	0.2166	-1.6460	1.7315	0.1902	0.1043
5.3	5119	0.0533	0.0427	-0.0041	0.1707	-0.9125	1.1079	0.1553	0.0726
1.5	1680	0.0638	0.0424	0.0153	0.0475	-0.6959	0.3072	0.0671	0.0148

Copyright © 2025 Texas Instruments Incorporated

5.4 Weibull Fit

Weibull-Fit and cross section plots for the INA1H94-SP at supply voltages of 5V and of 18V are shown in Figure 5-12 and Figure 5-13, respectively. The Weibull equation used for the fits is shown in Equation 1, and the parameters used to plot the Weibull fits are provided in Table 5-9. For each of the supply voltages, the total number of transients and the run fluences are used to calculate the mean (σ_{MEAN}), upper bound (σ_{UB}), and lower bound (σ_{LB}) cross section (as discussed in Appendix B) at 95% confidence interval. As events were still recorded as low as 1.5MeV-cm^2 / mg, SET onset is assumed to fall between that point and 0MeV-cm^2 / mg. For the calculations below, onset was modeled as 0MeV-cm^2 / mg.

$$\sigma = \sigma_{SAT} \times \left(1 - e^{\left(\frac{LET - Onset}{w}\right)^{S}}\right) \quad (1)$$

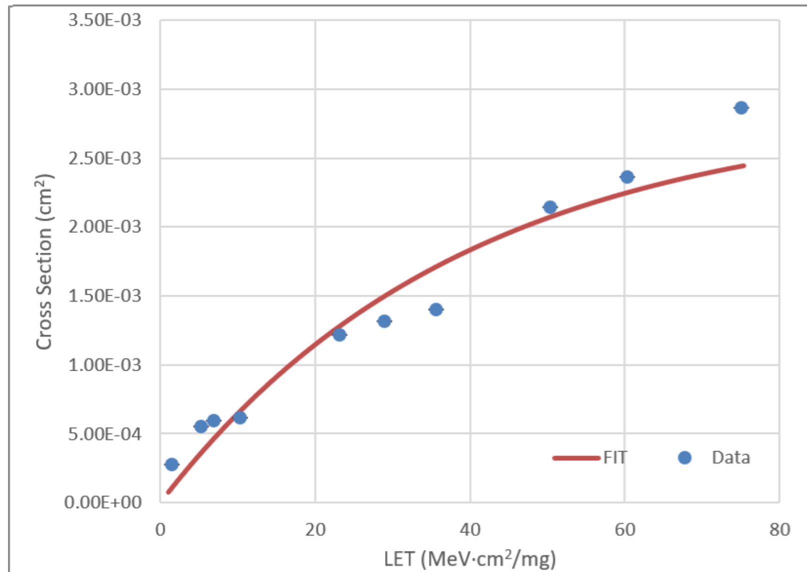

Figure 5-12. Cross Section and Weibull Fit for 5V Supply

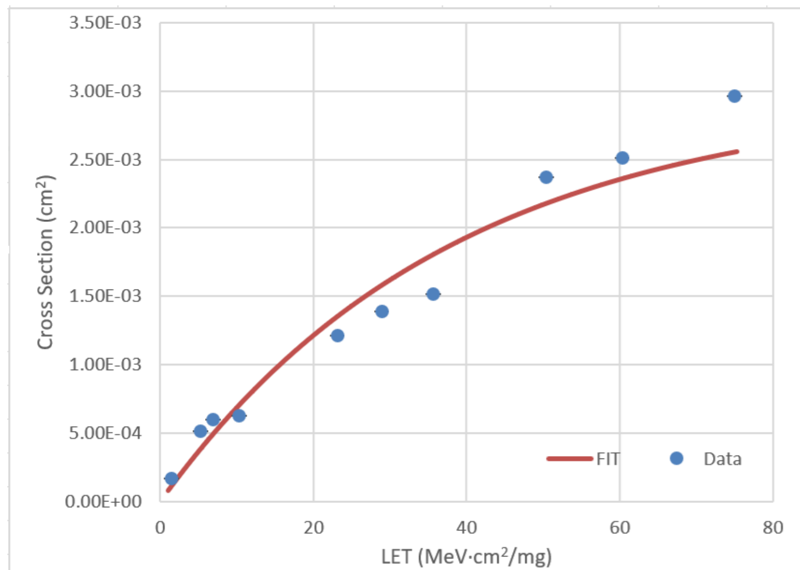

Figure 5-13. Cross Section and Weibull Fit for 18V Supply

Copyright © 2025 Texas Instruments Incorporated

Table 5-7. Cross Section and Weibull Fit Data: 5V Supply

Energy (MeV-cm^2 /mg)	Ion	Fluence (Ions/cm^2)	Total Events	σ_{LB} (cm^2/Device)	σ_{MEAN} (cm^2/Device)	FIT	Residual	Residual^2	σ_{UB} (cm^2/Device)	UB Error	LB Error
75	^{169}Tm	1.00E+07	28617.16667	0.988441309	2.86E-03	0.002443	4.18E-04	1.75E-07	2.90E-03	3.33E-05	-9.86E-01
60.3	^{129}Xe	1.00E+07	23605.25	0.987272789	2.36E-03	0.002252	1.09E-04	1.18E-08	2.39E-03	3.03E-05	-9.85E-01
50.4	^{129}Xe	1.00E+07	21430.5	0.986655751	2.14E-03	0.002076	6.73E-05	4.52E-09	2.17E-03	2.89E-05	-9.85E-01
35.6	^{86}Kr	1.00E+07	14023.25	0.983498983	1.40E-03	0.001713	-3.11E-04	9.66E-08	1.43E-03	2.34E-05	-9.82E-01
28.9	^{86}Kr	1.00E+07	13193.75	0.982989777	1.32E-03	0.001498	-1.78E-04	3.18E-08	1.34E-03	2.27E-05	-9.82E-01
23.1	^{86}Kr	1.00E+07	12167.75	0.982289425	1.22E-03	0.001279	-6.23E-05	3.88E-09	1.24E-03	2.18E-05	-9.81E-01
10.3	^{40}Ar	1.00E+07	6172.285714	0.975160705	6.17E-04	0.000664	-4.70E-05	2.21E-09	6.33E-04	1.56E-05	-9.75E-01
6.9	^{40}Ar	1.00E+07	5961.428571	0.974703522	5.96E-04	0.000464	1.32E-04	1.75E-08	6.11E-04	1.53E-05	-9.74E-01
5.3	^{40}Ar	1.00E+07	5519.857143	0.973727589	5.52E-04	0.000364	1.88E-04	3.55E-08	5.67E-04	1.47E-05	-9.73E-01
1.5	^{16}O	1.00E+07	2796.2	0.963204685	2.80E-04	0.000108	1.72E-04	2.95E-08	2.90E-04	1.05E-05	-9.63E-01

Table 5-8. Cross Section and Weibull Fit Data, 18V Supply

Energy (MeV-cm^2 /mg)	Ion	Fluence (Ions/cm^2)	Total Events	σ_{LB} (cm^2/Device)	σ_{MEAN} (cm^2/Device)	FIT	Residual	Residual^2	σ_{UB} (cm^2 / Device)	UB Error	LB Error
75	^{169}Tm	1.00E+07	29634	0.988646473	2.96E-03	0.002552	4.12E-04	1.7E-07	3.00E-03	3.39E-05	-9.86E-01
60.3	^{129}Xe	1.00E+07	25118	0.987671002	2.51E-03	0.002357	1.55E-04	2.39E-08	2.54E-03	3.13E-05	-9.85E-01
50.4	^{129}Xe	1.00E+07	23690.75	0.987295722	2.37E-03	0.002177	1.92E-04	3.7E-08	2.40E-03	3.03E-05	-9.85E-01
35.6	^{86}Kr	1.00E+07	15127.5	0.984127247	1.51E-03	0.001802	-2.89E-04	8.38E-08	1.54E-03	2.43E-05	-9.83E-01
28.9	^{86}Kr	1.00E+07	13921	0.983456488	1.39E-03	0.001578	-1.86E-04	3.47E-08	1.42E-03	2.33E-05	-9.82E-01
23.1	^{86}Kr	1.00E+07	12129.75	0.982261796	1.21E-03	0.00135	-1.37E-04	1.87E-08	1.23E-03	2.18E-05	-9.81E-01
10.3	^{40}Ar	1.00E+07	6242.142857	0.975322081	6.24E-04	0.000704	-7.94E-05	6.3E-09	6.40E-04	1.57E-05	-9.75E-01
6.9	^{40}Ar	1.00E+07	5963.428571	0.974707749	5.96E-04	0.000492	1.04E-04	1.09E-08	6.12E-04	1.53E-05	-9.74E-01
5.3	^{40}Ar	1.00E+07	5118.857143	0.972722298	5.12E-04	0.000386	1.26E-04	1.59E-08	5.26E-04	1.42E-05	-9.72E-01
1.5	^{16}O	1.00E+07	1680.125	0.952677146	1.68E-04	0.000115	5.33E-05	2.84E-09	1.76E-04	8.22E-06	-9.53E-01

Copyright © 2025 Texas Instruments Incorporated

Table 5-9. Weibull Fit Parameters

Parameter	Value for 5V Supply	Value for 18V Supply
σ_{SAT} (cm^2)	2.86×10^{-3}	2.96×10^{-3}
Onset (MeV-cm^2 /mg)	0	0
w	39	38
s	1	1
Sum ($Residual^2$)	3.786×10^{-7}	4.006×10^{-7}

6 Summary

Single-event effects of the INA1H94-SP radiation-hardened, high common-mode voltage difference amplifier were studied. The device was shown through characterization to be latch-up immune up to surface LET_{EFF} = 75MeV-cm^2 / mg and T = 125°C.

A MSU Results Appendix

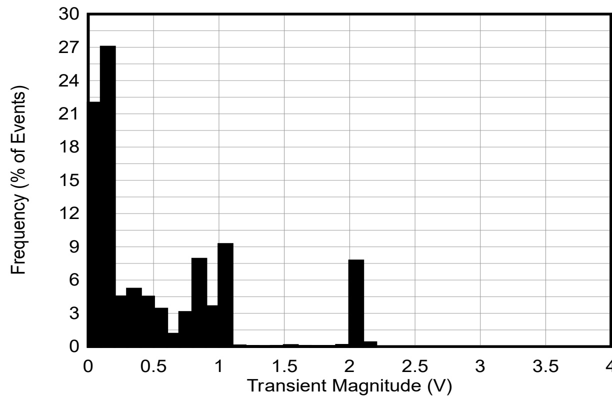

Figure A-1. Transient Event Magnitude Histogram, 5V Supply, LETeff = 75MeV-cm^2 / mg

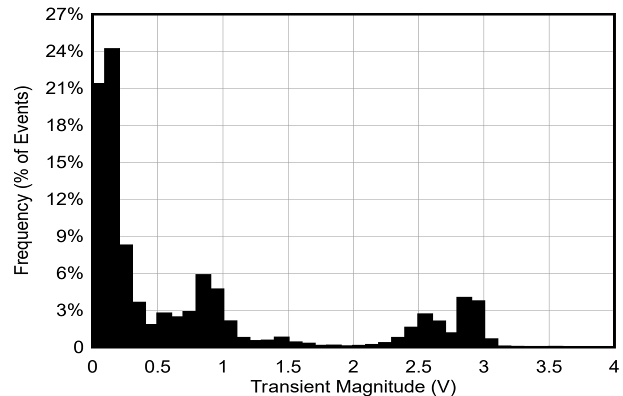

Figure A-2. Transient Event Magnitude Histogram, 18V Supply, LETeff = 75MeV-cm^2 / mg

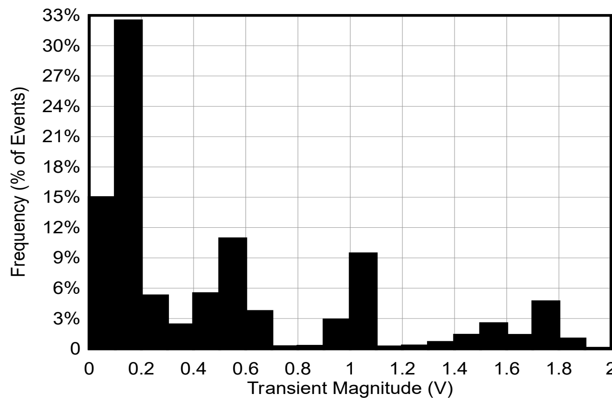

Figure A-3. Transient Event Magnitude Histogram, 5V Supply, LETeff = 50.4MeV-cm^2 / mg

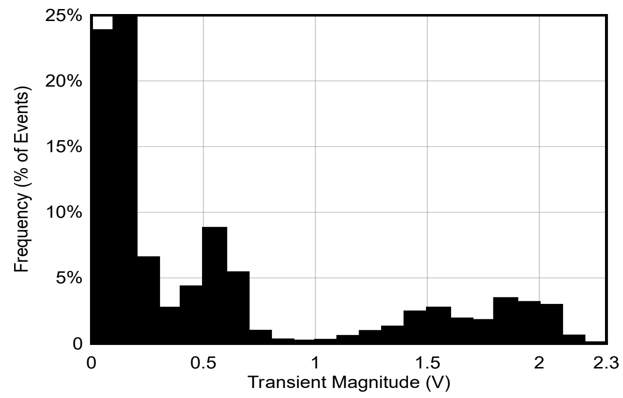

Figure A-4. Transient Event Magnitude Histogram, 18V Supply, LETeff = 50.4MeV-cm^2 / mg

Copyright © 2025 Texas Instruments Incorporated

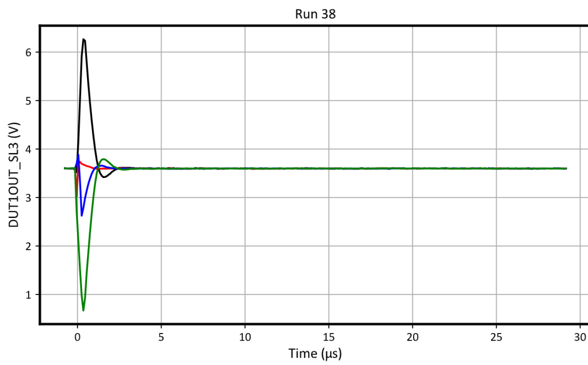

Figure A-5. 18V Supply, LETeff = 70MeV-cm^2 / mg, Typical Output Transients

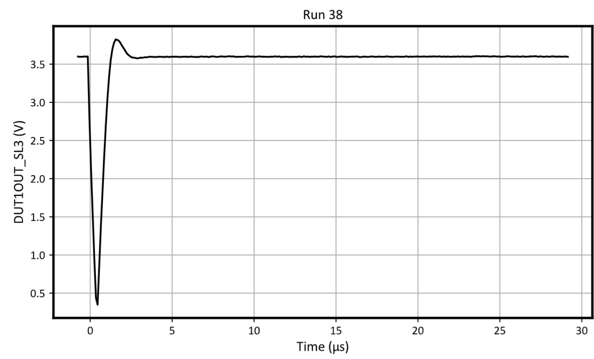

Figure A-6. 18V Supply, LETeff = 75MeV-cm^2 / mg, Large Neg Out Transient

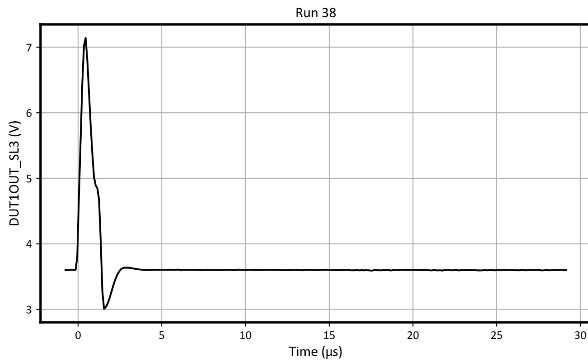

Figure A-7. 18V Supply, LETeff = 75MeV-cm^2 / mg, Large Pos Out Transient

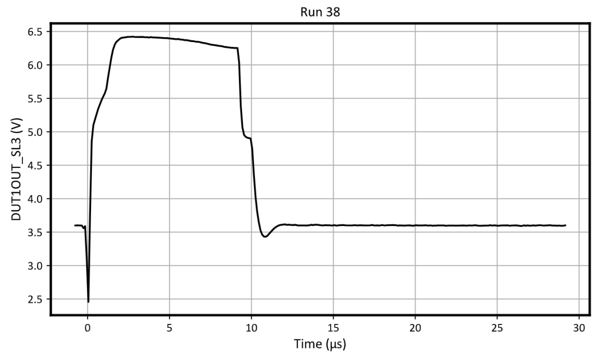

Figure A-8. 18V Supply, LETeff = 75MeV-cm^2 / mg, Long Pos Out Transient

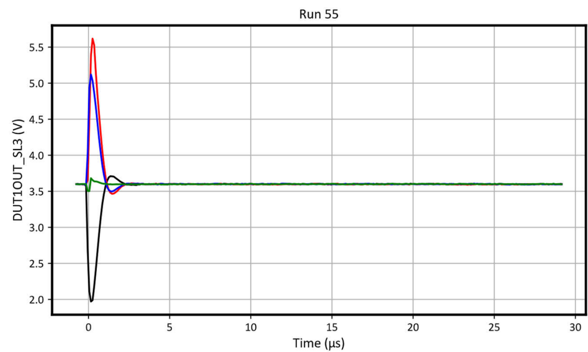

Figure A-9. 18V Supply, LETeff = 50.4MeV-cm^2 / mg, Typical Output Transients

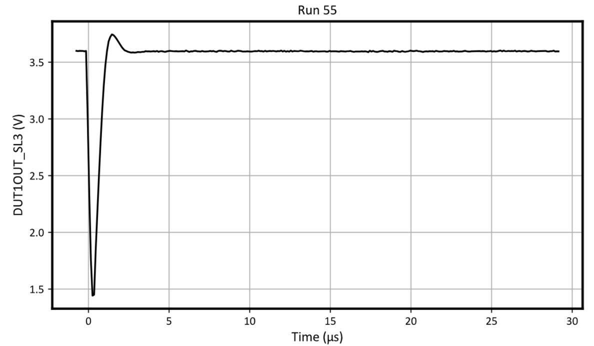

Figure A-10. 18V Supply, LETeff = 50.4MeV-cm^2 / mg, Large Neg Out Transient

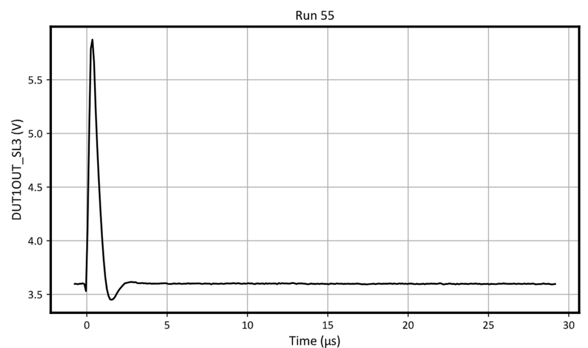

Figure A-11. 18V Supply, LETeff = 50.4MeV-cm^2 / mg, Large Pos Out Transient

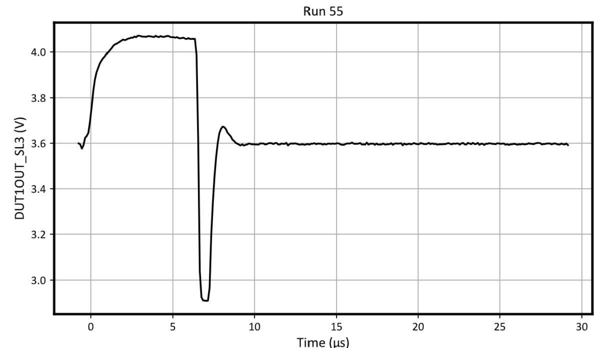

Figure A-12. 18V Supply, LETeff = 50.4MeV-cm^2 / mg, Long Pos Out Transient

Copyright © 2025 Texas Instruments Incorporated

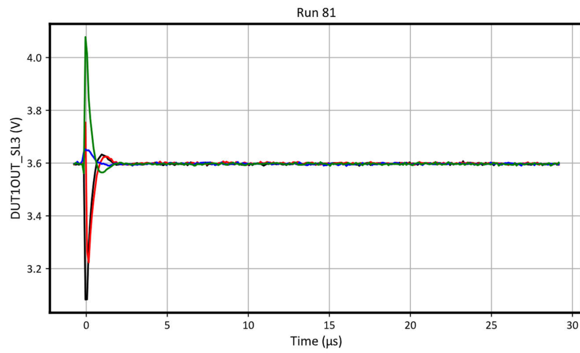

Figure A-13. 18V Supply, LETeff = 35.6MeV-cm^2 / mg, Typical Output Transients

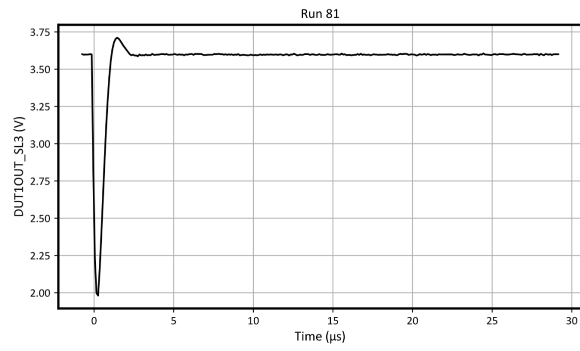

Figure A-14. 18V Supply, LETeff = 35.6MeV-cm^2 / mg, Large Neg Out Transient

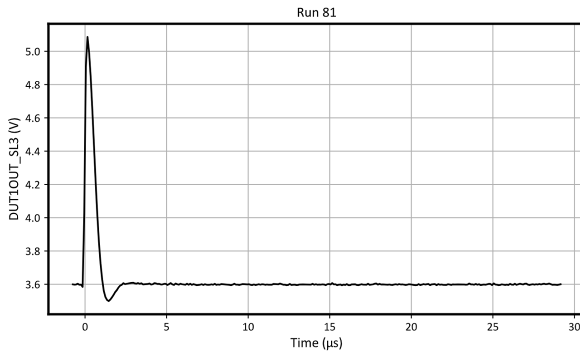

Figure A-15. 18V Supply, LETeff = 35.6MeV-cm^2 / mg, Large Pos Out Transient

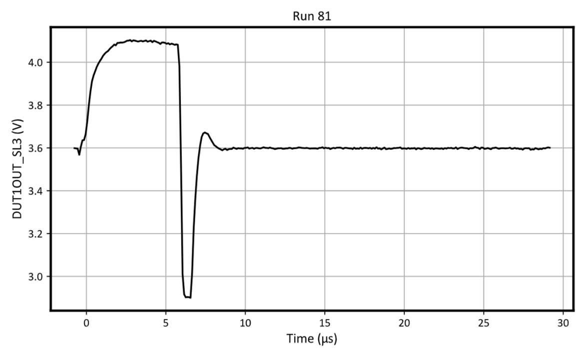

Figure A-16. 18V Supply, LETeff = 35.6MeV-cm^2 / mg, Long Pos Out Transient

Copyright © 2025 Texas Instruments Incorporated

B Confidence Interval Calculations

For conventional products where hundreds of failures are seen during a single exposure, one can determine the average failure rate of parts being tested in a heavy-ion beam as a function of fluence with high degree of certainty and reasonably tight standard deviation, and as a result, have confidence that the calculated cross-section is accurate.

With radiation-hardened parts however, determining the cross-section is difficult because often few or no failures are observed during an entire exposure. Determining the cross-section using an average failure rate with standard deviation is no longer a viable option, and the common practice of assuming a single error occurred at the conclusion of a null-result can result in a greatly underestimated cross-section.

In cases where observed failures are rare or non-existent, the use of confidence intervals and the chi-squared distribution is indicated. The chi-squared distribution is particularly designed for the determination of a reliability level when the failures occur at a constant rate. In the case of SEE testing where the ion events are random in time and position within the irradiation area, a failure rate is expected that is independent of time (presuming that parametric shifts induced by the total ionizing dose do not affect the failure rate), and as a result, the use of chi-squared statistical techniques is valid (because events are rare, an exponential or Poisson distribution is used).

In a typical SEE experiment, the device-under-test (DUT) is exposed to a known, fixed fluence (ions / cm^2) while the DUT is monitored for failures. This is analogous to fixed-time reliability testing and, more specifically, time-terminated testing where the reliability test is terminated after a fixed amount of time whether or not a failure has occurred (in the case of SEE tests fluence is substituted for time and hence is a fixed fluence test [(6)]). Calculating a confidence interval specifically provides a range of values which is likely to contain the parameter of interest (the actual number of failures per fluence). Confidence intervals are constructed at a specific confidence level. For example, a 95% confidence level implies that if a given number of units were sampled numerous times and a confidence interval estimated for each test, the resulting set of confidence intervals can bracket the true population parameter in about 95% of the cases.

To estimate the cross-section from a null-result (no fails observed for a given fluence) with a confidence interval, start with the standard reliability determination of lower-bound (minimum) mean-time-to-failure for fixed-time testing (an exponential distribution is assumed) in Equation 2:

$$MTTF = \frac{2nT}{\chi^2_{2(d+1);100\left(1-\frac{\alpha}{2}\right)}} \quad (2)$$

Where:

- *MTTF* is the minimum (lower-bound) mean-time-to-failure,
- *n* is the number of units tested (presuming each unit is tested under identical conditions),
- *T* is the test time,
- and χ^2 is the chi-square distribution evaluated at 100(1 – α / 2) confidence level
- *d* is the degrees-of-freedom (the number of failures observed).

With slight modification for our purposes we invert the inequality and substitute *F* (fluence) in the place of *T* as shown in Equation 3:

$$MFTF = \frac{2nF}{\chi^2_{2(d+1);100\left(1-\frac{\alpha}{2}\right)}} \quad (3)$$

Copyright © 2025 Texas Instruments Incorporated

Where:

- *MFTF* is mean-fluence-to-failure
- *F* is the test fluence
- X^2 is the chi-square distribution evaluated at 100(1 – α / 2) confidence
- *d* is the degrees-of-freedom (the number of failures observed).

The inverse relation between *MTTF* and failure rate is mirrored with the *MFTF*. Thus the upper-bound cross-section is obtained by inverting the *MFTF* as shown in Equation 4:

$$\sigma = \frac{\chi^2_{2(d+1);100\left(1-\frac{\alpha}{2}\right)}}{2nF} \tag{4}$$

Assume that all tests are terminated at a total fluence of 10^6 ions/cm^2. Assume there are a number of devices with different performances that are tested under identical conditions. Assume a 95% confidence level (σ = 0.05). Note that as *d* increases from 0 events to 100 events, the actual confidence interval becomes smaller, which indicates that the range of values of the true value of the population parameter (in this case, the cross-section) is approaching the mean value + 1 standard deviation. As more events are observed, the statistics are improved such that uncertainty in the actual device performance is reduced.

Table B-1. Experimental Example Calculation of MFTF and σ Using a 95% Confidence Interval (1)

Degrees-of-Freedom (d)	2(d + 1)	X^2 at 95%	Calculated Cross-Section (cm^2)		
			Upper-Bound at 95% Confidence	Mean	Average + Standard Deviation
0	2	7.38	3.69E–06	0.00E+00	0.00E+00
1	4	11.14	5.57E–06	1.00E–06	2.00E–06
2	6	14.45	7.22E–06	2.00E–06	3.41E–06
3	8	17.53	8.77E–06	3.00E–06	4.73E–06
4	10	20.48	1.02E–05	4.00E–06	6.00E–06
5	12	23.34	1.17E–05	5.00E–06	7.24E–06
10	22	36.78	1.84E–05	1.00E–05	1.32E–05
50	102	131.84	6.59E–05	5.00E–05	5.71E–05
100	202	243.25	1.22E–04	1.00E–04	1.10E–04

(1) Using a 95% confidence interval for several different observed results (d = 0, 1, 2,…100 observed events during fixed-fluence tests) assuming 10^6 ions / cm^2 for each test. Note that as the number of observed events increases the confidence interval approaches the mean.

Copyright © 2025 Texas Instruments Incorporated

C References

1. M. Shoga and D. Binder, Theory of Single Event Latchup in Complementary Metal-Oxide Semiconductor Integrated Circuits, *IEEE Trans. Nucl. Sci., Vol. 33(6)*, Dec. 1986, pp. 1714-1717.
2. G. Bruguier and J. M. Palau, "Single particle-induced latchup", *IEEE Trans. Nucl. Sci., Vol. 43(2)*, Mar. 1996, pp. 522-532.
3. Texas A&M University, *Texas A&M University Cyclotron Institute Radiation Effects Facility*, webpage.
4. Michigan State University, *MSU Facility for Rare Isotope Beams*, webpage.
5. Ziegler, James F. *The Stopping and Range of Ions in Matter*, webpage.
6. D. Kececioglu, “Reliability and Life Testing Handbook”, Vol. 1, PTR Prentice Hall, New Jersey, 1993, pp. 186-193.
7. Vanderbilt University, *ISDE CRÈME-MC*, webpage.
8. A. J. Tylka, J. H. Adams, P. R. Boberg, et al.,"CREME96: A Revision of the Cosmic Ray Effects on Micro-Electronics Code", *IEEE Trans. on Nucl. Sci., Vol. 44(6)*, Dec. 1997, pp. 2150-2160.
9. A. J. Tylka, W. F. Dietrich, and P. R. Boberg, "Probability distributions of high-energy solar-heavy-ion fluxes from IMP-8: 1973-1996", *IEEE Trans. on Nucl. Sci.,Vol. 44(6)*, Dec. 1997, pp. 2140-2149.

Copyright © 2025 Texas Instruments Incorporated

IMPORTANT NOTICE AND DISCLAIMER

TI PROVIDES TECHNICAL AND RELIABILITY DATA (INCLUDING DATA SHEETS), DESIGN RESOURCES (INCLUDING REFERENCE DESIGNS), APPLICATION OR OTHER DESIGN ADVICE, WEB TOOLS, SAFETY INFORMATION, AND OTHER RESOURCES “AS IS” AND WITH ALL FAULTS, AND DISCLAIMS ALL WARRANTIES, EXPRESS AND IMPLIED, INCLUDING WITHOUT LIMITATION ANY IMPLIED WARRANTIES OF MERCHANTABILITY, FITNESS FOR A PARTICULAR PURPOSE OR NON-INFRINGEMENT OF THIRD PARTY INTELLECTUAL PROPERTY RIGHTS.

These resources are intended for skilled developers designing with TI products. You are solely responsible for (1) selecting the appropriate TI products for your application, (2) designing, validating and testing your application, and (3) ensuring your application meets applicable standards, and any other safety, security, regulatory or other requirements.

These resources are subject to change without notice. TI grants you permission to use these resources only for development of an application that uses the TI products described in the resource. Other reproduction and display of these resources is prohibited. No license is granted to any other TI intellectual property right or to any third party intellectual property right. TI disclaims responsibility for, and you will fully indemnify TI and its representatives against, any claims, damages, costs, losses, and liabilities arising out of your use of these resources.

TI’s products are provided subject to TI’s Terms of Sale or other applicable terms available either on ti.com or provided in conjunction with such TI products. TI’s provision of these resources does not expand or otherwise alter TI’s applicable warranties or warranty disclaimers for TI products.

TI objects to and rejects any additional or different terms you may have proposed.

Mailing Address: Texas Instruments, Post Office Box 655303, Dallas, Texas 75265

Copyright © 2025, Texas Instruments Incorporated